Dirhodium(II) tetrakis[*N*,*N*-dimethyl-2-pyrrolidone-5(*S*)-carboxamide]. Structural effects on enantioselection in metal carbene transformations

Michael P. Doyle* and William R. Winchester
Department of Chemistry, Trinity University, San Antonio, TX 78212 (USA)

Stanley H. Simonsen* and Ratna Ghosh
Department of Chemistry and Biochemistry, University of Texas, Austin, TX 78712 (USA)

(Received January 10, 1994)

Abstract

The preparation and structural characterization of dirhodium(II) tetrakis[*N*,*N*-dimethyl-2-pyrrolidone-5(*S*)-carboxamide], $Rh_2(5S\text{-DMAP})_4$, a new sterically-demanding catalyst for enantioselective metal carbene transformations, is described. The pyrrolidone ligands are arrayed around the dirhodium(II) core with two oxygen and two nitrogen donor atoms, each oriented *cis*, bound to each octahedral rhodium. The crystal structure of this compound has been determined to be that of $Rh_2(5S\text{-DMAP})_4(CH_3CN)_2 \cdot CH_3CN \cdot 6H_2O$: space group $P2_12_12_1$ with cell constants $a = 12.685(4)$, $b = 15.050(3)$, $c = 24.035(4)$ Å; $V = 4588.5(1.9)$ Å^3, $Z = 4$, $R = 0.0316$, Rh–Rh distance = 2.4538(5) Å. Decreased activity for diazodecomposition catalyzed by $Rh_2(5S\text{-DMAP})_4$ is observed, and enantiocontrol for cyclopropanation and carbon–hydrogen insertion is lower than expected by analogy to the corresponding dirhodium(II) tetrakis[methyl 2-pyrrolidone-5(*S*)-carboxylate], $Rh_2(5S\text{-MEPY})_4$. Electronic stabilization of the intermediate metal carbene is absent in reactions catalyzed by $Rh_2(5S\text{-DMAP})_4$.

Key words: Crystal structures; Enantioselectivity; Cyclopropanation; Rhodium carboxamidate complexes; Carbene complexes; Dinuclear complexes; Carbon–hydrogen insertion

Introduction

We have recently reported extraordinary enantioselectivity in metal carbene transformations of diazoacetate esters catalyzed by dirhodium(II) tetrakis[methyl 2-pyrrolidone-5(*S*)-carboxylate], $Rh_2(5S\text{-MEPY})_4$, and its enantiomeric form, $Rh_2(5R\text{-MEPY})_4$ [1–7]. These catalysts were constructed by ligand displacement on dirhodium(II) tetraacetate with the chiral amide ligand. The only isomer of the tetrasubstituted dirhodium(II) formed was that in which two oxygen and two nitrogen donor atoms, each oriented *cis*, were bound to each octahedral rhodium. Similar high selectivities, enhanced for intramolecular carbon–hydrogen insertion reactions [8], have been achieved with the oxazolidinone analog of $Rh_2(5S\text{-MEPY})_4$, dirhodium(II) tetrakis[methyl 2-oxazolidinone-4(*S*)-carboxylate], $Rh_2(4S\text{-MEOX})_4$, but not with those whose substituents are benzyl, $Rh_2(4S\text{-BNOX})_4$, or isopropyl, $Rh_2(4S\text{-IPOX})_4$ [1–5]. Significant improvement in enantiocontrol was observed, however, when phenyl was the substituent instead of benzyl, and the influence of this catalyst, $Rh_2(4S\text{-PHOX})_4$, although not as great as the carboxylate-substituted catalysts, was reported to be the result of greater steric control of the transition states for carbenoid processes [9].

The transformation for which these catalysts have proven to be the most effective are intramolecular cyclopropanation [1, 3, 10] and carbon–hydrogen insertion reactions [1, 4, 8] of diazoesters (e.g. eqns. (1) and (2)). Among simple substrates enantiometric excesses (e.e.) greater than 90% have been achieved, and increasing the substitution on the diazoacetate often leads to even higher % e.e. values. This pattern further suggests the influence of steric control on enantioselectivity. However, steric influence alone cannot explain the extraordinary selectivity provided by chiral dirhodium(II) catalysts with carboxylate attachments, $Rh_2(MEPY)_4$ and $Rh_2(MEOX)_4$. Their influence has been attributed to interaction of the ligand's carbonyl oxygen with the carbene carbon which is viewed as

*Authors to whom correspondence should be addressed.

SSDI 0020-1693(94)03872-L

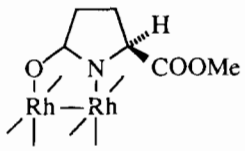

$Rh_2(5S\text{-MEPY})_4$

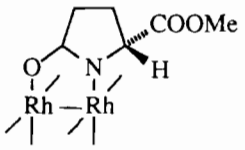

$Rh_2(5R\text{-MEPY})_4$

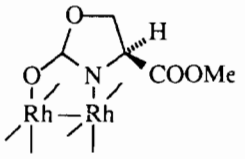

$Rh_2(4S\text{-MEOX})_4$

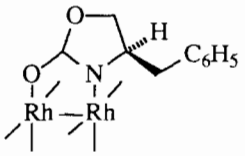

$Rh_2(4S\text{-BNOX})_4$

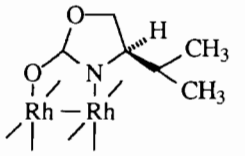

$Rh_2(4S\text{-IPOX})_4$

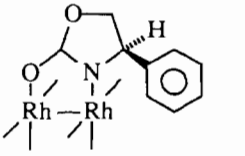

$Rh_2(4S\text{-PHOX})_4$

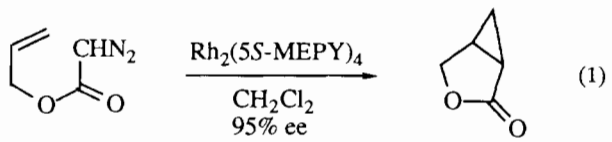

(1)

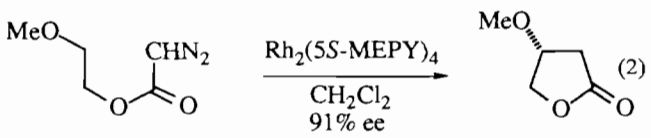

(2)

stabilizing the transition state for electrophilic reactions as well as further orienting the carbene for greater enantiocontrol [1, 17].

The design of new ligands for dirhodium(II) that could further enhance enantioselectivity in metal carbene transformations brought us to *N,N*-dimethyl-2-pyrrolidone-5(*S*)-carboxamide. The greater steric bulk of the dimethylamido group relative to methoxy and the increased basicity of the amide carbonyl oxygen were expected to have a substantial influence on enantioselectivity in reactions catalyzed by the resulting dirhodium(II) compound, $Rh_2(5S\text{-DMAP})_4$. We now report the synthesis, structure and catalytic effectiveness of $Rh_2(5S\text{-DMAP})_4$.

Experimental

General

Dirhodium(II) tetraacetate was obtained commercially or prepared from rhodium(III) chloride hydrate [11]. (−)-2-Pyrrolidone-5(*S*)-carboxylic acid was recrystallized from ethanol prior to use: $[\alpha]_D^{22} = -10°$ (H_2O, $c = 0.97$), and its methyl ester was prepared as previously described [1]. *d*-(+)-Menthyl diazoacetate and *l*-(−)-menthyl diazoacetate [12] were prepared from their corresponding diazoacetoacetate esters by deacylation in aqueous acetonitrile with 3.0 equiv. of lithium hydroxide [13]. 3-Methyl-2-buten-1-yl diazoacetate and 2-methoxy-1-ethyl diazoacetate were prepared by similar methods [1]. Chlorobenzene, dichloromethane and 1,2-dichloroethane were distilled from calcium hydride prior to use.

N,N-Dimethyl-2-pyrrolidone-5(S)-carboxamide

A 100 ml one-neck, round bottom flask, cooled to −78 °C, was charged with 50 ml of anhydrous, freshly distilled dimethylamine. Methyl 2-pyrrolidone-5(*S*)-carboxylate (5.5 g, 38 mmol) was added to this solution, the flask was sealed with a rubber septum, and the resulting solution was allowed to warm to room temperature. When the reaction was complete (24 h, as indicated by a NMR spectrum of a sample removed from the reaction solution), the flask was again cooled to −78 °C, the septum was replaced with a still head, and excess dimethylamine was removed by distillation. The residue was a white solid that was recrystallized from ethyl acetate. The resulting white solid (4.2 g, 27 mmol, 70% yield) had a m.p. of 114–115 °C and $[\alpha]_D^{22} = -37.2°$ (H_2O, $c = 1.164$); lit $[\alpha]_D^{23} = -33.5°$ (H_2O, $c = 2$) [14]. ^1H NMR ($CDCl_3$, 300 MHz): δ 6.89 (s, 1H), 4.56 (dd, $J = 8.0$, 4.6 Hz, 1H), 3.09 (s, 3H), 3.02 (s, 3H), 2.52–2.27 (m, 3H), 2.20–2.03 (m, 1H). ^{13}C NMR ($CDCl_3$, 75 MHz): δ 178.2, 171.2, 53.9, 36.4, 35.9, 29.4, 24.9.

Dirhodium(II) tetrakis[N,N-dimethyl-2-pyrrolidone-5(S)-carboxamide], $Rh_2(5S\text{-DMAP})_4$

Rhodium(II) acetate (200 mg, 0.452 mmol), *N,N*-dimethyl-2-pyrrolidinone-5(*S*)-carboxamide (1.0 g, 6.4 mmol) and 20 ml of anhydrous chlorobenzene were combined in a 50 ml one-neck, round bottom flask fitted with a Soxhlet extraction apparatus into which was placed a thimble containing 5 g of an oven-dried mixture of 2 parts Na_2CO_3 and one part sand. The

solution turned blue soon after mixing the reactants at room temperature, and HPLC analysis on a μ-Bondapak-CN column (2% acetonitrile in methanol) suggested the presence of several ligand substitution products. The resulting solution was heated and maintained at reflux temperature for 16 h, and then chlorobenzene was removed under reduced pressure. Purification of the blue solid by chromatography on a column containing 10 g of J.T. Baker Bondapak-CN capped silica in methanol yielded unreacted ligand in the first 100 ml elution. Subsequent elution with 2% acetonitrile in methanol (vol./vol.) caused an immediate color change in the dirhodium(II) band from blue to red and its rapid passage through the column. The entire red band was collected as one fraction, and the solvent was removed under reduced pressure. Recrystallization from acetonitrile (0.5 ml/100 mg) yielded bright red crystals that were isolated by filtration and washed with a minimal amount of isopropyl alcohol and pentane (155 mg, 0.190 mmol, 42% yield). ^{1}H NMR ($CDCl_3$, 300 MHz): δ 4.52 (dd, $J=9.9$, 6.8 Hz, 2H), 4.42 (dd, $J=8.0$, 5.8 Hz, 2H), 3.37 (s, 6H), 3.07 (s, 6H), 3.05 (s, 6H), 2.92 (s, 6H), 2.72–2.53 (m, 4H), 2.50–2.37 (m, 4H), 2.18–1.86 (m, 8H). ^{13}C NMR ($CDCl_3$, 75 MHz): δ 187.0, 185.0, 175.6, 174.1, 66.7, 61.5, 37.7, 36.9, 36.7, 35.8, 33.3, 31.8, 27.5, 25.6. $[\alpha]_D^{23} = -260 \pm 10°$ (CH_3CN, $c = 6.8 \times 10^{-2}$); $[\alpha]^{23}_{Hg/365} = -741 \pm 20°$ (CH_3CN, $c = 6.8 \times 10^{-2}$).

X-ray crystallography for Rh_2(5S-DMAP)$_4$

Crystals of Rh_2(5*S*-DMAP)$_4$ suitable for X-ray crystallography were grown from an acetonitrile solution over a period of one month. From these crystals the data crystal was a red block of approximate dimensions $0.37 \times 0.33 \times 0.35$ mm. The data were collected at 183 K on a Siemens R3 diffractometer equipped with a Nicolet LT-2 low-temperature device and using a graphite monochromator with Mo Kα radiation ($\lambda = 0.7107$ Å). Lattice parameters were obtained from the least-squares refinement of 50 reflections with $18.71 < 2\theta < 23.78$. The data were collected using the ω-scan technique with a 2θ range from 4.0 to 60.0°, with a 1° ω-scan at 6–12° min ($h = 0$ to 18, $k = 0$ to 22, $l = 0$ to 34; $h = 0$ to 18, $k = -22$ to 0, $l = -34$ to 0). A total of 14713 reflections was collected of which 8181 were unique. Four reflections (1, 2, 13; 2, 5, 9; 3, 4, 11; 4, 5, 1) were remeasured every 96 reflections to monitor instrument and crystal stability. A smoothed curve of the intensities of these check reflections was used to scale the data. The scaling factor ranged from 0.998 to 1.1750. The data were corrected for Lp effects and absorption. The absorption correction was applied based on measured crystal faces using SHELXTL-PLUS [15]. The data reduction and decay correction were applied using the Nicolet XRD SHELXTL-PLUS software package. The structure was solved by direct methods [15] and refined by full-matrix least-squares. In all, 558 parameters were refined.

The non-H atoms were refined with anisotropic thermal parameters. Hydrogen atom positions at the ligands and the acetonitriles were calculated for idealized positions (C–H = 0.96 Å, N–H = 0.90 Å) and were not refined. Hydrogens on O22 and O24 were observed in the difference Fourier map. One hydrogen each was found for the two water oxygens (O21 and O23), and no hydrogens were found for O25 and O26. Full geometry of probable hydrogen bonds (1, 4, 6, 10, 11 and 12) could not be ascertained. Sigma (I) was estimated from counting statistics; $\sigma(I) = [(I_{peak} + I_{background})^{1/2} \times (\text{scan rate})]$. The data were corrected for secondary extinction. The correction is of the form: $F_{corr} = F_{calc}/[(1 + 0.6(2) \times 10^{-7}) - (F_{calc})^2/\sin^2\theta]^{1/4}$. The scattering factors for the non-H atoms were taken from Cromer and Mann [16], with the anomalous-dispersion corrections taken from the work of Cromer and Liberman [17]. The scattering factors for the H atoms were obtained from Stewart *et al.* [18]. Values used to calculate the linear absorption coefficient are from the International Tables for X-ray Crystallography [19]. All figures were generated using SHELXTL-PLUS. The crystallographic data are listed in Table 1. Fractional coordinates and equivalent isotropic thermal parameters (Å^2) for the non-hydrogen atoms of Rh_2(5*S*-DMAP)$_4$ structure are given in Table 2. Selected bonds lengths and angles are given in Table 3.

Catalytic diazodecomposition reactions

Reactions were performed as previously described [1] by controlled addition of the diazoester in either dichloromethane or 1,2-dichloroethane to a refluxing solution of catalyst (1.0 mol%) and alkene (if intermolecular cyclopropanation reaction) in the refluxing solvent. After addition was complete, the reaction solution was filtered through a 1 cm silica plug, and the plug was eluted with additional solvent. The solvent was removed under reduced pressure, and the residue was purified by column chromatography. Menthyl 2-phenylcyclopropane-carboxylates were analyzed by GC on a 30-m capillary methylsilicone column which provided baseline diastereoisomer resolutions. Enantiomeric excesses were determined from product analyses on a Chiraldex G-TA capillary column.

Reactions performed in refluxing dichloromethane were incomplete even after long addition times; unreacted diazoester was recovered as the major or sole product. However, these same reactions occurred without inhibition in refluxing dichloroethane. Neither catalytic activity nor reactivity was improved by heating the catalyst overnight in a vacuum oven.

TABLE 1. Crystallographic data for $(C_7H_{11}N_2O_2)_4Rh_2(CH_3CN)_2 \cdot CH_3CN \cdot 6H_2O$

Formula	$Rh_2C_{34}H_{65}N_{11}O_{14}$
Formula weight	1057.75
Space group	$P2_12_12_1$
a (Å)	12.685(4)
b (Å)	15.050(3)
c (Å)	24.035(4)
V (Å^3)	4588.5(1.9)
Z	4
Crystal system	orthorhombic
ρ_{calc} (g/cc)	1.528
Crystal size (mm)	$0.37 \times 0.33 \times 0.35$
Radiation, λ (Å)	Mo Kα, 0.07107
Temperature (°C)	−90
2θ Range (°)	4.0–60.0
Reflections measured	14713
Unique reflections	8181
Reflections rejected	920 $[F_o < 4(\sigma(F_o))]$
R_{int}	0.0316
Transmission factor[a] range	0.5822–0.6553
Secondary extinction[b] correction factor	$0.6(2) \times 10^{-7}$
$R(F)$[c]	0.035 (7261 reflections)
$R_w(F)$	0.041 (8181 reflections)
Goodness of fit	1.219
Max. $\lvert\Delta/\sigma\rvert$	0.003
Min., max. peaks (e/Å^3)	−0.771, 0.562

[a]Absorption correction was based on measured crystal faces. [b]The correction for secondary extinction is of the form: $F_{corr} = F_{calc}/[(1+X)(F_{calc})^2/\sin^2\theta]^{1/4}$ where X is the correction factor. [c]The function $\Sigma w(|F_o| - |F_c|)^2)$ was minimized, where $\omega = 1/(s(F_o)^2 + (0.02F)^2)$ and $s(F_o) = \{0.5kI^{1/2}[s(I)^2 + (0.02I)^2]^{1/2}\}$ with $I = (I_{peak} - I_{background}) \times$ scan rate. The factor 0.02 was used to downweight intense reflections and to account for instrument instability; k is the correction due to Lp effects, absorption and decay.

Results and discussion

All four acetates of dirhodium(II) acetate were replaced by *N*,*N*-dimethyl-2-pyrrolidone-5(*S*)-carboxamide using the methodology originally developed for the preparation of dirhodium(II) tetrakis(acetamidate) [20] and subsequently employed to synthesize Rh_2(5*S*-MEPY)$_4$ and other chiral dirhodium(II) carboxamides [1]. Both the carbon and proton NMR spectra of Rh_2(5*S*-DMAP)$_4$ suggest the (2,2-*cis*) ligand geometry. This ligand orientation is confirmed by the X-ray crystal structure of the bis-acetonitrile complex (Fig. 1). Viewed along the Rh(2)–Rh(1) bond axis, the nearer carboxamide substituents have a counter-clockwise orientation, whereas the farther carboxamides have a clockwise orientation, consistent with the *S*-configuration (Fig. 2). Each of the carboxamide substituents is positioned so that the dimethylamido group is pointed away from the dirhodium(II) core, and each of them has the expected planar geometry. The Rh–Rh, Rh–O and Rh–N bond lengths of the Rh_2(5*S*-DMAP)$_4$ structure are very close to those reported for Rh_2(5*R*-MEPY)$_4$ [1]. The Rh–Rh–N(pyrrolidone) bond angles average 85.28(11)°, while the Rh–Rh–O bond angles average 89.65(8)°. However, whereas the pyrrolidone rings of Rh_2(5*R*-MEPY)$_4$ are only slightly twisted, those of Rh_2(5*S*-DMAP)$_4$ are considerably distorted (Fig. 1): ligand a, puckered between a twist and envelope conformation; ligand b, twist conformation; ligands c and d, envelope. The acetonitrile ligand of Rh(2) is bonded with a linear atomic array for Rh(2)–N(12)–C(13) (178°), whereas that of Rh(1) has a Rh(1)–N(15)–C(16) bond angle of only 163°.

X-ray crystallographic analysis of Rh_2(5*S*-DMAP)$_4$ revealed six water molecules in the crystal structure. The carbonyl oxygens of two ligands, O(10c), O(11c) and O(10d), O(11d), form hydrogen bonds with four water molecules; the other two water molecules form bridges to the first three in what appears to be a cluster (see 'Supplementary material') which extends to a molecule of acetonitrile that is incorporated into the crystalline lattice.

The catalytic activity for diazodecomposition of Rh_2(5*S*-DMAP)$_4$ stands in sharp contrast with that of the analogous Rh_2(5*S*-MEPY)$_4$. Intramolecular cyclopropanation reactions of 3-methyl-2-buten-1-yl diazoacetate or intramolecular carbon–hydrogen insertion reactions of 2-methoxy-1-ethyl diazoacetate performed with Rh_2(5*S*-DMAP)$_4$ in refluxing dichloromethane led to the recovery of unreacted diazoester. With ethyl diazoacetate and styrene in refluxing dichloromethane, the cyclopropanation product ethyl 2-phenylcyclopropane-carboxylate was isolated in only 47% yield (eqn. (3)) with a *cis*:*trans* isomer ratio of 34:66 and enantiomeric excesses of 38% (1*S*, 2*R*) and 22% (1*S*, 2*S*). In contrast, with Rh_2(5*S*-MEPY)$_4$ these isomeric cy-

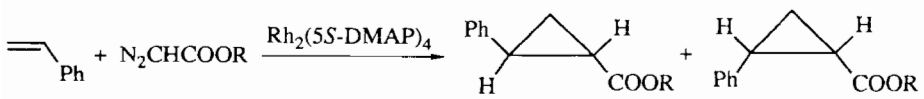

(3)

R = Et, 40°C (47% yield)	66 (22% ee)	34 (38% ee)
R = *l*-Menthyl, 40°C (27% yield)	63 (2% de)	37 (13% de)
R = *l*-Menthyl, 83°C (75% yield)	64 (1% de)	36 (15% de)
R = *d*-Menthyl, 83°C (83% yield)	58 (7% de)	42 (33% de)

TABLE 2. Fractional coordinates and equivalent isotropic thermal parameters (Å^2) for the non-hydrogen atoms of $(C_7H_{11}N_2O_2)_4Rh_2(CH_3CN)_2 \cdot CH_3CN \cdot 6H_2O$

Atom	x	y	z	U
Rh1	0.10468(2)	−0.00625(2)	0.108890(10)	0.01636(7)
Rh2	0.19699(2)	−0.12569(2)	0.158450(10)	0.01617(7)
N1A	0.1772(3)	−0.1958(2)	0.0884(2)	0.0218(9)
C2A	0.1376(3)	−0.1611(3)	0.0431(2)	0.0230(11)
C3A	0.1172(4)	−0.2306(3)	−0.0011(2)	0.0330(14)
C4A	0.1200(4)	−0.3167(3)	0.0319(3)	0.041(2)
C5A	0.1835(3)	−0.2926(3)	0.0848(2)	0.0239(11)
C6A	0.2985(4)	−0.3237(3)	0.0789(2)	0.0261(11)
N7A	0.3234(3)	−0.4053(3)	0.0984(2)	0.0355(13)
C8A	0.4308(4)	−0.4378(4)	0.0914(3)	0.051(2)
C9A	0.2488(5)	−0.4652(4)	0.1255(3)	0.049(2)
O10A	0.3635(3)	−0.2779(3)	0.0543(2)	0.0415(12)
O11A	0.1164(3)	−0.0792(2)	0.03546(12)	0.0243(8)
N1B	−0.0259(3)	−0.0762(2)	0.1238(2)	0.0217(9)
C2B	−0.0272(3)	−0.1481(3)	0.1547(2)	0.0234(11)
C3B	−0.1317(3)	−0.1952(4)	0.1532(3)	0.0366(15)
C4B	−0.1854(5)	−0.1518(4)	0.1037(3)	0.060(2)
C5B	−0.1239(3)	−0.0661(3)	0.0920(2)	0.0273(12)
C6B	−0.1845(3)	0.0168(3)	0.1107(2)	0.0278(12)
N7B	−0.2347(3)	0.0645(3)	0.0721(2)	0.0366(13)
C8B	−0.2901(5)	0.1446(4)	0.0890(3)	0.055(2)
C9B	−0.2389(6)	0.0457(5)	0.0134(3)	0.057(2)
O10B	−0.1897(3)	0.0345(3)	0.1603(2)	0.0418(11)
O11B	0.0511(2)	−0.1764(2)	0.18346(13)	0.0245(8)
N1C	0.3289(2)	−0.0692(2)	0.1289(2)	0.0200(9)
C2C	0.3292(3)	0.0052(3)	0.0999(2)	0.0215(10)
C3C	0.4372(4)	0.0287(3)	0.0789(2)	0.0332(14)
C4C	0.4970(4)	−0.0580(4)	0.0855(2)	0.039(2)
C5C	0.4345(3)	−0.1094(3)	0.1303(2)	0.0243(11)
C6C	0.4882(3)	−0.0963(3)	0.1861(2)	0.0267(12)
N7C	0.5561(3)	−0.1587(3)	0.2036(2)	0.0308(11)
C8C	0.6205(5)	−0.1389(4)	0.2532(3)	0.048(2)
C9C	0.5747(4)	−0.2442(3)	0.1761(2)	0.0339(14)
O10C	0.4744(3)	−0.0268(2)	0.2130(2)	0.0349(10)
O11C	0.2481(2)	0.0529(2)	0.09057(13)	0.0238(8)
N1D	0.0938(3)	0.0519(2)	0.18399(14)	0.0205(9)
C2D	0.1383(3)	0.0191(3)	0.2288(2)	0.0224(10)
C3D	0.1089(4)	0.0706(3)	0.2806(2)	0.0297(12)
C4D	0.0076(4)	0.1180(3)	0.2614(2)	0.0327(13)
C5D	0.0269(3)	0.1266(3)	0.1976(2)	0.0220(10)
C6D	0.0819(3)	0.2152(3)	0.1870(2)	0.0237(11)
N7D	0.0236(3)	0.2886(3)	0.1818(2)	0.0289(11)
C8D	0.0732(4)	0.3758(3)	0.1829(3)	0.043(2)
C9D	−0.0925(4)	0.2901(3)	0.1829(2)	0.0352(14)
O10D	0.1799(3)	0.2194(2)	0.1861(2)	0.0362(11)
O11D	0.1995(3)	−0.0485(2)	0.23024(11)	0.0224(7)
N12	0.2786(3)	−0.2340(3)	0.2044(2)	0.0258(10)
C13	0.3187(3)	−0.2893(3)	0.2297(2)	0.0321(13)
C14	0.3673(5)	−0.3601(6)	0.2611(4)	0.077(3)
N15	0.0285(3)	0.1082(3)	0.0658(2)	0.0277(11)
C16	0.0121(3)	0.1767(3)	0.0474(2)	0.0290(13)
C17	−0.0063(5)	0.2642(4)	0.0236(3)	0.048(2)
C18	0.7855(10)	0.5584(9)	0.0637(6)	0.176(8)
C19	0.8872(10)	0.5214(7)	0.0683(3)	0.083(4)
N20	0.9700(7)	0.4939(7)	0.0706(3)	0.094(3)
O21	0.2491(4)	0.1649(4)	−0.0020(2)	0.074(2)
O22	0.3726(3)	0.1374(3)	0.2059(2)	0.0443(13)
O23	0.2552(5)	0.2869(5)	0.0817(3)	0.095(3)
O24	0.6220(6)	0.3547(5)	0.0963(3)	0.109(3)
O25	0.4543(5)	0.2521(5)	0.1213(3)	0.089(2)
O26	0.3509(5)	−0.0423(5)	0.3123(2)	0.093(3)

For anisotropic atoms, the U value is U_{eq}, calculated as $U_{eq} = \frac{1}{3} \Sigma_i \Sigma_j U_{ij} a_i^* a_j^* A_{ij}$ where A_{ij} is the dot product of the ith and jth direct space unit cell vectors.

clopropane compounds were formed in higher yield with a *cis:trans* isomer ratio of 44:56 and enantiomeric excesses of 33% (1*S*, 2*R*) and 58% (1*S*, 2*S*) [2]. Under the same conditions, cyclopropanation of styrene using *l*-methyl diazoacetate was also incomplete. However, in refluxing dichloroethane reactions of *d*- and *l*-menthyl diazoacetate with styrene catalyzed by Rh_2(5*S*-DMAP)$_4$ went to completion, cyclopropane product yields were relatively high, and diastereomeric excesses were those reported in eqn. (3). Stereodifferention for *d*- and *l*-menthyl diazoacetate reactions with styrene, with greatly different levels of diastereocontrol from the *d*- and *l*-menthyl esters, is similar to that found with Rh_2(4*S*-BNOX)$_4$, Rh_2(4*S*-IPOX)$_4$ and Rh_2(4*S*-PHOX)$_4$ [1, 2, 9] and unlike the small differences found with the Rh_2(MEPY)$_4$ catalysts [21]. No significant difference in activity or selectivity in Rh_2(5*S*-DMAP)$_4$ promoted reactions was found when the catalyst was heated in a vacuum oven to remove volatile ligands like acetonitrile.

Intramolecular cyclopropanation of 3-methyl-2-buten-1-yl diazoacetate (eqn. (4)) and intramolecular carbon–hydrogen insertion (eqn. (2)) reactions catalyzed by Rh_2(5*S*-DMAP)$_4$ occurred without undue complications at 83 °C in refluxing 1,2-dichloroethane. The 44% e.e. obtained from eqn. (4) can be compared with 77% e.e. for the same product achieved with Rh_2(5*S*-MEPY)$_4$ in refluxing benzene [6]. Similarly, the product from C–H insertion (eqn. (2)) was obtained in only 30% e.e. compared to more than twice that selectivity with Rh_2(5*S*-MEPY)$_4$. Overall, enantioselectivities from the use of Rh_2(5*S*-DMAP)$_4$ are considerably lower than those from the use of Rh_2(5*S*-MEPY)$_4$.

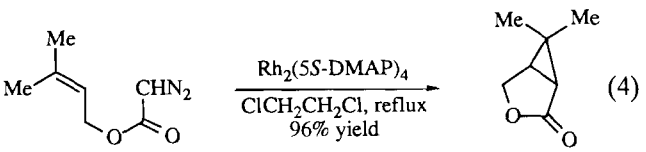

(4)

44% ee (1*S*,5*R*)

The decreased activity and selectivity of Rh_2(5*S*-DMAP)$_4$, relative to Rh_2(5*S*-MEPY)$_4$, towards diazodecomposition and metal carbene transformations are surprising. The open side of the catalyst not encumbered by carboxamide attachments would appear to have allowed ready access by diazoesters to the active rhodium center (Fig. 2). Increased selectivity based on either or both steric effects and electronic stabilization of the intermediate carbene is not observed. Diazodecomposition by Rh_2(5*S*-DMAP)$_4$ generally requires much higher temperatures than those routinely employed with Rh_2(5*S*-MEPY)$_4$, and this lower activity is commonly attributed to steric effects [22]. The rigidity of Rh_2(5*S*-DMAP)$_4$, which is suggested by the distortion of the

TABLE 3. Selected bond distances (Å) and angles (°) for $(C_7H_{11}N_2O_2)_4Rh_2(CH_3CN)_2 \cdot CH_3CN \cdot 6H_2O$[a]

Bond distances					
Rh(2)–Rh(1)	2.4538(5)	N(1c)–Rh(2)	2.007(3)	C(4a)–C(3a)	1.521(7)
O(11a)–Rh(1)	2.084(3)	O(11d)–Rh(2)	2.080(3)	C(5a)–C(4a)	1.548(7)
N(1b)–Rh(1)	1.996(3)	N(12)–Rh(2)	2.224(4)	C(6a)–C(5a)	1.539(6)
O(11c)–Rh(1)	2.073(3)	C(2a)–N(1a)	1.308(6)	N(7a)–C(6a)	1.352(6)
N(1d)–Rh(1)	2.011(3)	C(5a)–N(1a)	1.462(5)	O(10a)–C(6a)	1.226(6)
N(15)–Rh(1)	2.231(4)	C(3a)–C(2a)	1.513(6)	C(8a)–N(7a)	1.458(7)
N(1a)–Rh(2)	2.002(4)	O(11a)–C(2a)	1.274(5)	C(9a)–N(7a)	1.460(8)
O(11b)–Rh(2)	2.090(3)				
Bond angles					
Rh(2)–Rh(1)–O(11a)	89.49(8)	O(11c)–Rh(1)–N(1d)	93.66(13)	C(5a)–C(4a)–C(3a)	104.04(4)
Rh(2)–Rh(1)–N(1b)	85.53(10)	O(11c)–Rh(1)–N(15)	87.13(13)	C(6a)–C(5a)–N(1a)	111.1(3)
Rh(2)–Rh(1)–O(11c)	89.94(9)	N(1d)–Rh(1)–N(15)	92.95(14)	C(6a)–C(5a)–N(4a)	110.2(4)
Rh(2)–Rh(1)–N(1d)	85.15(10)	N(15)–Rh(1)–Rh(2)	176.40(10)	N(1a)–C(5a)–C(4a)	104.7(4)
O(11a)–Rh(1)–N(1b)	86.20(13)	C(2a)–N(1a)–C(5a)	111.7(4)	N(7a)–C(6a)–O(10a)	121.4(4)
O(11a)–Rh(1)–O(11c)	89.07(12)	C(2a)–N(1a)–Rh(2)	122.5(3)	N(7a)–C(6a)–C(5a)	117.7(4)
O(11a)–Rh(1)–N(1d)	173.98(12)	C(5a)–N(1a)–Rh(2)	124.6(3)	O(10a)–C(6a)–C(5a)	120.7(4)
O(11a)–Rh(1)–N(15)	92.55(13)	C(3a)–C(2a)–O(11a)	122.1(4)	C(8a)–N(7a)–C(9a)	116.7(4)
N(1b)–Rh(1)–O(11c)	173.48(13)	C(3a)–C(2a)–N(1a)	112.0(4)	C(8a)–N(7a)–C(6a)	118.9(4)
N(1b)–Rh(1)–N(1d)	90.64(15)	O(11a)–C(2a)–N(1a)	125.9(4)	C(9a)–N(7a)–C(6a)	124.4(4)
N(1b)–Rh(1)–N(15)	97.56(14)	C(4a)–C(3a)–C(2a)	102.6(4)	N(12)–Rh(2)–Rh(1)	179.07(15)

[a]Estimated standard deviations in the least significant digit are given in parentheses.

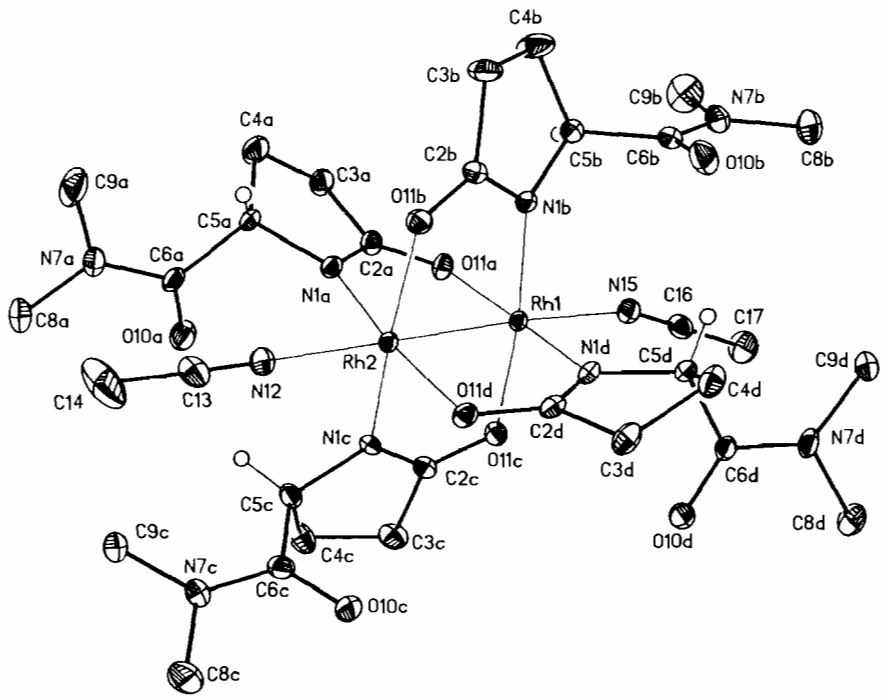

Fig. 1. View of $Rh_2(5S\text{-DMAP})_4(CH_3CN)_2$ with a numbering scheme showing the nearly octahedral coordination around the Rh atoms. Thermal ellipsoids are scaled to the 30% probability level.

pyrrolidone rings and in the bending of one acetonitrile ligand, can be used to rationalize these results. Consistent with this structural rigidity, we were unable to prepare the tetramethyleneamido analog of $Rh_2(5S\text{-DMAP})_4$ under the same reaction conditions but even longer reaction times.

Whereas steric interference which restricts access of diazocarbonyl compounds to the metal center is normally associated with ligands that surround the metal center on at least three sides [22], the present results suggest that this interference is more subtle. The proximity of a *N*,*N*-dimethylcarboxamido group to the approaching diazocarbonyl compound, which inhibits optimal alignment for electrophilic addition by rhodium, is one probable cause of the decreased reactivity of $Rh_2(5S\text{-DMAP})_4$. The substantial double diastereoselectivity

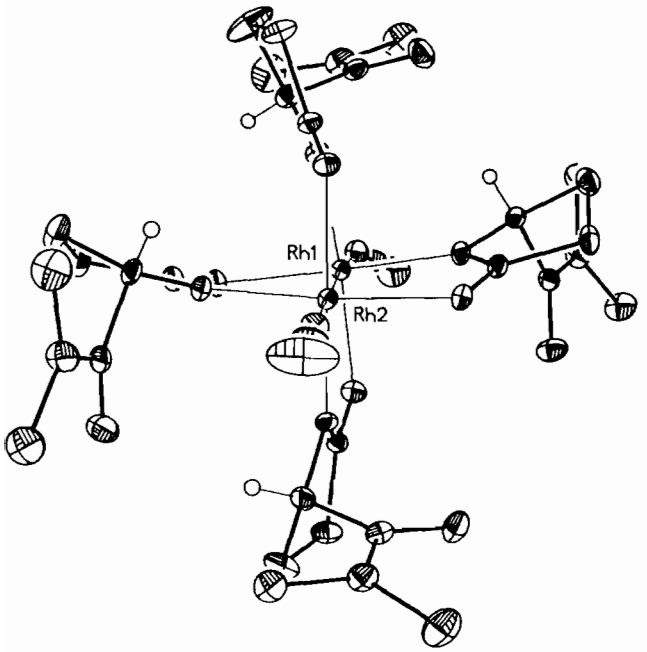

Fig. 2. The view direction of $Rh_2(5S\text{-DMAP})_4(CH_3CN)_2$ is down the Rh–Rh axis.

observed with $Rh_2(5S\text{-DMAP})_4$ (eqn. (3)), but not with $Rh_2(5S\text{-MEPY})_4$ [21], further suggests that the principal factor responsible for enantiocontrol with $Rh_2(5S\text{-MEPY})_4$, that is, electronic stabilization of the intermediate metal carbene by the pendant carboxylate group, is absent in reactions catalyzed by $Rh_2(5S\text{-DMAP})_4$. Overall, including $Rh_2(5S\text{-DMAP})_4$, the direction often taken to produce larger bulkier ligands for rhodium in catalytic metal carbene transformations has not proven to offer any significant advantage in catalytic activity or enantioselectivity [22, 23].

Supplementary material

For the crystal structure of $Rh_2(C_7H_{11}N_2O_2)_4(CH_3CN)_2 \cdot CH_3CN \cdot 6H_2O$: anisotropic thermal parameters for the non-hydrogen atoms (2 pages), positional and isotropic thermal parameters for the H atoms (2 pages), bond lengths and angles for the non-H atoms (3 pages), bond lengths and angles for the H atoms (3 pages), views of $Rh_2(5S\text{-DMAP})_4(CH_3CN)_2 \cdot CH_3CN \cdot 6H_2O$ showing the atom labelling scheme (2 pages), and a unit cell packing diagram (1 page) are available on request from author S.H.S.

Acknowledgements

Support for this research by the National Science Foundation and the Robert A. Welch Foundation to M.P.D. is gratefully acknowledged. S.H.S. and R.G. are grateful to the Robert A. Welch Foundation for their support. We thank J. van Hal for preliminary results.

References

1 M.P. Doyle, W.R. Winchester, J.A.A. Hoorn, V. Lynch, S.H. Simonsen and R. Ghosh, *J. Am. Chem. Soc., 115* (1993) 9968.
2 M.P. Doyle, B.D. Brandes, A.P. Kazala, R.J. Pieters, M.B. Jarstfer, L.M. Watkins and C.T. Eagle, *Tetrahedron Lett., 31* (1990) 6613.
3 M.P. Doyle, R.J. Pieters, S.F. Martin, R.E. Austin, C.J. Oalmann and P. Müller, *J. Am. Chem. Soc., 113* (1991) 1423.
4 M.P. Doyle, A. van Oeveren, L.J. Westrum, M.N. Protopopova and T.W. Clayton, Jr., *J. Am. Chem. Soc., 113* (1991) 8982.
5 M.N. Protopopova, M.P. Doyle, P. Müller and D. Ene, *J. Am. Chem. Soc., 114* (1992) 2755.
6 M.P. Doyle, M.Y. Eismont, D.E. Bergbreiter and H.N. Gray, *J. Org. Chem., 57* (1992) 6103.
7 M.P. Doyle, *Recl. Trav. Chim. Pays-Bas, 110* (1991) 305.
8 M.P. Doyle, M.N. Protopopova, W.R. Winchester and K.L. Daniel, *Tetrahedron Lett., 33* (1992) 7819.
9 M.P. Doyle, W.R. Winchester, M.N. Protopopova, P. Müller, G. Bernardinelli, D. Ene and S. Motallebi, *Helv. Chim. Acta, 76* (1993) 2227.
10 S.F. Martin, D.J. Oalmann and S. Liras, *Tetrahedron Lett., 33* (1992) 6727.
11 G.A. Rampel, P. Legdins, H. Smith and G. Wilkinson, *Inorg. Synth., 13* (1972) 90.
12 H. Fritschi, U. Leutenegger and A. Pfaltz, *Helv. Chim. Acta, 71* (1988) 1553.
13 M.P. Doyle, L.J. Westrum, W.N.E. Wolthuis, M.M. See, W.P. Boone, V. Bagheri and M.M. Pearson, *J. Am. Chem. Soc., 115* (1993) 958.
14 R.B. Angrev and V.K. Smith, *J. Org. Chem., 21* (1956) 1540.
15 G.M. Sheldrick, *SHELXTL-PLUS* (Version 4.11), Siemens X-ray Analytical Instruments, Inc., Madison, WI, USA, 1991.
16 D.T. Cromer and J.B. Mann, *Acta Crystallogr., Sect. A, 24* (1968) 321.
17 D.T. Cromer and D. Liberman, *J. Chem. Phys., 53* (1970) 1891.
18 R.F. Stewart, E.R. Davidson and W.T. Simpson, *J. Phys. Chem., 42* (1965) 3175.
19 *International Tables for X-ray Crystallography,* Vol. IV, Kynoch, Birmingham, UK, 1974, p. 55.
20 M.P. Doyle, V. Bagheri, T.J. Wandless, N.K. Harn, D.A. Brinker, C.T. Eagle and K.-L. Loh, *J. Am. Chem. Soc., 112* (1990) 1906.
21 M.P. Doyle, M.N. Protopopova, B.D. Brandes, H.M.L. Davies, N.J.S. Huby and J.K. Whitesell, *Synlett,* (1993) 151.
22 H.J. Callot, A.-M. Albrecht-Gary, M.A. Joubbeh, B. Metz and F. Metz, *Inorg. Chem., 28* (1989) 3633.
23 S. O'Malley and T. Kodadek, *Organometallics, 11* (1992) 2299.